On the Detection of High Redshift Black Holes with ALMA through CO and H_2 Emission

Marco Spaans

Kapteyn Astronomical Institute, P.O. Box 800, 9700 AV Groningen, The Netherlands

spaans@astro.rug.nl

and

Rowin Meijerink

Astronomy Department, University of California, Berkeley, CA 94720, United States

ABSTRACT

Many present-day galaxies are known to harbor supermassive, $\geq 10^6$ $M_\odot$, black holes. These central black holes must have grown through accretion from less massive seeds in the early universe. The molecules CO and H_2 can be used to trace this young population of accreting massive black holes through the X-ray irradiation of ambient gas. The X-rays drive a low-metallicity ion-molecule chemistry that leads to the formation and excitation of CO and H_2 in $100 < T \leq 1,000$ K gas. H_2 traces very low metallicity gas, $\sim 10^{-3}$ solar or less, while some pollution by metals, $\sim 10^{-2}$ solar or more, must have taken place to form CO. Strong CO $J > 15$ and H_2 S(0) & S(1) emission is found that allows one to constrain ambient conditions. Comparable line strengths cannot be produced by FUV or cosmic ray irradiation. Weak, but perhaps detectable, H_3^+ (2,2)$\rightarrow$(1,1) emission is found and discussed. The models predict that black hole masses larger than 10^5 $M_\odot$ can be detected with ALMA, over a redshift range of 5-20, provided that the black holes radiate close to Eddington.

Subject headings: cosmology: theory – galaxies: black holes –ISM: clouds – ISM: molecules – molecular processes

1. Introduction

Central to the study of galaxy evolution is the formation and evolution of the supermassive black holes in their nuclei. Accretion onto these black holes can provide the energy source

for active galactic nuclei, which in turn impact the evolution of galaxies (Silk 2005). The processes believed to play a role in the formation of seed black holes, from which large black holes may form through accretion, involve 1) dynamical friction and collision processes in dense young stellar clusters (Portegies Zwart et al. 2004); 2) seeds as the remnants of popIII stars (e.g., Bromm et al. 1999, Abel et al. 2000, Yoshida et al. 2003); 3) accretion of low angular momentum material and gravitational instability in primordial disks (e.g., Koushiappas, Bullock & Dekel 2004; Lodato & Natarajan 2007); and 4) the (singular) collapse of massive pre-galactic halos (Bromm & Loeb 2003; Spaans & Silk 2006).

The growth of these seed black holes to larger sizes involves accretion that roughly follows an Eddington rate and requires the incorporation of feedback effects (Silk & Rees 1998, Wyithe & Loeb 2003, Di Matteo, Springel & Hernquist 2005). See Pelupessy, Di Matteo & Ciardi (2007) for an asessment on the difficulties that seed black holes have to grow at the Eddingtion rate. Understanding the growth of these black holes is also important because there appears to be a scaling relation between bulge and black hole mass, with about 10^{-3} of the bulge mass tied up in the central black holes (Magorrian et al. 1998, Ferrarese & Merritt 2000, Häring & Rix 2004). In this work, it is investigated how one can observe a population of these putative black holes in the early universe, at redshifts $z = 5-20$, through high temperature molecular lines that are driven by X-rays and that are accessible to the Atacama Large Millimeter Array (ALMA), which covers the 300 μm to 3 mm wavelength range.

2. Model Description

We consider a high redshift halo which already contains, by assumption, a seed black hole. Suppose further that an initially metal-free hydrogen gas is cooled by Lyman α to $T \sim 10^4$ K and settles in the center of a halo close to the black hole. Part of the gas is likely to experience a period of popIII star formation. If popIII star formation occurs, then the short life times of primordial stars ensure that the accreted gas is quickly polluted by a modest amount of dust and metals. If no star formation takes place, then the gas will remain metal-free. In either case, the accretion process will lead to the emission of X-rays that impact the thermal, ionization an chemical balance of the gas in the halo, leading to an X-ray dominated region (XDR, Maloney et al. 1996; Meijerink & Spaans 2005). For simplicity the black hole is taken to radiate at the Eddington luminosity.

For a baryonic number density $\rho_b/m_H = 3 \times 10^{-7}$ cm^{-3} today, hydrogen mass m_H, halo masses of $M_h = 10^7 - 10^9$ $M_\odot$ and a characteristic size scale of $L = (3M_h/4\pi\rho)^{1/3}$, one has a typical mean density and column of $n_0 = 0.05[(1+z)/10]^3$ cm^{-3} and $N_0 =$

$10^{22}[(1+z)/10]^2(M_h/10^9 M_\odot)^{1/3}$ cm^{-2}, respectively. The work of Mo, Mao & White (1988) shows that the subsequent formation of a disk occurs, with a collapse factor of $1/\lambda = 0.05$. This yields densities that exceed $10^{2.5}$ cm^{-3} within 1 kpc. The above cosmology provides the boundary conditions for the ambient density and column density of individual models, and the metallicity is put in by hand.

The models of Meijerink & Spaans (2005) and Meijerink et al. (2007) are used to compute the thermal, chemical and ionization balance of the irradiated gas self-consistently, for one-dimensional constant density slabs of gas. The multi-zone escape probability method of Poelman & Spaans (2005, 2006) has been used to compute the line intensities presented here. The same radiative transfer is performed in relevant atomic (fine-structure) and molecular (rotational and vibrational) cooling lines. Cloud type "A" from Meijerink et al. (2007, their Table 1) is adopted, which is 1 pc in size. The interested reader is referred to the cited papers for a detailed description of all physical processes involved. There are four free parameters in the models: hydrogen density, hydrogen column density, metallicity and X-ray flux. The latter parameterizes unknowns like the accretion rate, turbulent viscosity and the spectral shape of the X-ray radiation. For definiteness, a power law radiation field with $E^{-0.9}$ is adopted for energies E between 1 and 100 keV, appropriate for a self-absorbed Seyfert nucleus. This slope, if it is between -1.1 and -0.7 does not significantly impact the chemistries of H_2, CO and H_3^+; see also Meijerink & Spaans (2005) for the case of a 1 keV thermal spectrum. Solar elemental abundance ratios are adopted. As long as [O/C]> 1 this does not influence the CO results. Chemical equilibrium is assumed. At densities of $\sim 10^5$ cm^{-3} and for high X-ray fluxes, collisional and radiative time scales are short compared to the free-fall time. The chemical network comprises a few thousand reactions between 154 species with sizes up to 4 atoms (Woodall et al. 2006). Polycyclic aromatic hydrocarbons and small grains are included in the charge balance and are assumed to scale with the elemental carbon abundance.

Following the above cosmology, we consider column densities of $10^{22} - 10^{24}$ cm^{-2} and densities of $n = 10^3 - 10^5$ cm^{-3}. The X-ray flux takes values of $F_X = 0.1 - 100$ erg s^{-1} cm^{-2}. Results are shown in the Figures 1, 2 and 3 for a density of 10^5 cm^{-3}. Values below this density but above 10^3 cm^{-3} were found to lead to similar signal strengths for H_2 and H_3^+. For CO, line intensities smaller by a factor of $\sim n/10^5$ were found. Recall that the Eddington luminosity is $L_{\rm edd} \approx 1.3 \times 10^{38} M/M_\odot$ erg s^{-1}. So $F_X \approx 100$ erg s^{-1} cm^{-2} corresponds to a 10^6 $M_\odot$ black hole that emits $\sim 10^{44}$ erg s^{-1} through a surface with a radius of about 100 pc. The level to which popIII star formation pollutes the center of the primodial galaxy with metals through supernova explosions is a free parameter. Metallicities between 10^{-3} and 1.0 solar are considered since 10^{-3} solar is quite like a zero-metallicity gas as far as H_2 and CO are concerned, and supersolar values appear unlikely for the bulk of the very high redshift

gas. Dust grains, with standard Milky Way properties (Mathis et al. 1977), are included and their abundance is assumed to scale with the overall metallicity. The velocity dispersion of the gas has a thermal contribution, equal to $\Delta V = 12.9(T/10^4)^{1/2}$ km/s, and a turbulent contribution, equal to $\Delta V = 5$ km/s, for individual gas clouds on the scale of 1 pc. In the dense gas considered here, turbulence is expected to be maintained at a level similar to that in active galaxies.

3. Results

The main goal is to compute the expected columns of H_2, CO and H_3^+, and their associated emission strengths. For simplicity, a fiducial column of $10^{23.5}$ cm^{-2} is adopted for the predicted line emissivities. This is driven by the theoretical considerations above, but also by recent observations of massive galaxies at $z \sim 2$ (Daddi et al. 2007a,b). A significant fraction (20-30%) of the systems appear to contain heavily obscured AGN with columns in excess of 10^{24} cm^{-2}. These massive systems appear to be a somewhat later stage of the concurrent bulge-black hole mass forming systems studied here. The X-ray luminosities of these lower redshift counterparts is $(1-4) \times 10^{43}$ erg s^{-1} in the 2-8 keV band. The precise value of the total obscuring hydrogen column does not impact our emissivity results as long as it exceeds 10^{23} cm^{-2}, i.e., includes all $T > 100$ K gas.

3.1. H_2 and H_3^+

In the absence of dust grains, H_2 is formed in the gas phase through the H^- route, $H^- + H \rightarrow H_2 + e^-$. This leads to high abundances of H_2, $10^{-2}-10^{-0.5}$, even for low metallicities (Figure 1). So, contrary to far-ultraviolet (FUV, 6-13.6 eV) illumination, X-ray irradiation constitutes a form of positive feedback for H_2 (Haiman et al. 1997). The models with a modest metallicity of $> 10^{-3}$, and thus dust grains, follow the H_2 formation prescription as in Cazaux & Spaans (2004), which includes both physisorbed and chemisorbed hydrogen atoms. The columns of H_2 that are reached at low metallicities are as large as 10^{23} cm^{-2}. This while temperatures exceed 100 K over the bulk of this column, and reach 10^3 K at its edge, sufficient to excite the ~ 500 K S(0) line at 28 μm and ~ 800 K S(1) line at 17 μm. The S(1) line is typically weaker than the S(0) line, while both lines are optically thin and in LTE. High molecular gas temperatures are reached in XDRs because of efficient ionization and Coulomb heating, rather than photo-electric heating from dust grains (Meijerink & Spaans 2005). Interestingly, an increase in metallicity decreases the H_2 line strength. This is a direct consequence of enhanced cooling in fine-structure lines and a lower resulting temperature.

Hence, the pure rotational H_2 lines are particularly well suited to detect the earliest stages of black hole accretion, prior to significant metal pollution by star formation. Metallicities below 10^{-3} were found to lead to quite similar H_2 emissivities since all H_2 is formed in the gas phase and fine-structure cooling is modest.

Figure 2 (see Section 4 for its details) shows rest frame line intensities of $\sim 10^{-1}$ erg s^{-1} cm^{-2} sr^{-1} at a metallicity of 10^{-3} solar. For the numbers below, the ALMA sensitivity tool on the ESO website has been used and the concordance model, with the latest WMAP3 results, is adopted. With a source size of $0.2''$, or 600 pc at $z = 15$, this yields a S(0) flux density of $39/(1+z)^3$ Jy, for a fiducial galaxy center velocity dispersion of 20 km/s (~ 200 pc from a $\sim 10^8 M_\odot$ central mass). For the S(0) line from $z = 15$, so at 0.45 mm, and for 10 km/s spectral resolution, this is detectable with ALMA (50 antennas, beam size = source size) at the 6σ level in 4 hours of integration. Hence, despite the fact that the line falls in the less sensitive band 9, spectrally resolved detection is possible. The pure rotational H_2 lines are intrinsically very bright, because of the strong contribution from the X-ray driven H^- route, and are accessible to ALMA for redshifts above 10, for S(0) 28 μm, and above 16 for S(1) 17 μm.

Figure 1, for a density of 10^5 cm^{-3}, shows that the H_3^+ abundance increases with ionization parameter F_X/n for metallicities below 10^{-2} of solar. A higher X-ray ionization rate leads to a larger H_3^+ abundance, through H_2 secondary ionizations, and boosts the formation rate H_2+$H_2^+ \rightarrow H_3^+$. The H_2 abundance is thus key since no H_3^+ can be formed without it. Too large values of F_X/n lead to a decrease in the H_3^+ abundance, driven by dissociative recombination.

The best candidate for an H_3^+ detection is the optically thin (2,2)$\rightarrow$(1,1) line at 95 μm, as suggested by Pan & Oka (1986). The critical density of the (2,2)$\rightarrow$(1,1) transition is about 2×10^3 cm^{-3} and the excitation energy ~ 150 K. Collisions between H_3^+ and electrons have been included in the non-thermal rotational excitation of H_3^+ (Faure et al. 2006). In all, Figure 2 shows that one reaches a maximum rest frame intensity of $\sim 10^{-6}$ erg s^{-1} cm^{-2} sr^{-1}, at low metallicity and strong X-ray irradiation, with typical abundances of $10^{-8} - 10^{-9}$. With a source size of $0.4''$, or about 1.8 kpc at $z = 9$, this yields a flux density of $9/(1+z)^3$ mJy, for a fiducial galaxy center velocity dispersion of 20 km/s. For $z = 10$ at 1 mm (from 95 μm), this is barely detectable with ALMA at the 3σ level, in 48 hours of integration (50 antennas, beam size = source size), and only if the line is unresolved.

3.2. CO

Any metallicity larger than 10^{-3} solar leads to significant, $\sim 10^{-8} - 10^{-6}$, abundances of CO. X-rays, because of their large energy, do not dissociate CO directly. FUV photons are produced through collisional excitation of H and H_2 by electrons, followed by radiative decay. This UV flux is generally modest and thus CO can survive even in strong X-ray radiation fields. Given the high molecular gas temperatures in XDRs, $10^2 - 10^3$ K, rotational levels with $J > 10$ are excited (Meijerink et al. 2006, 2007). This very high J CO emission requires densities $> 10^{4.5}$ cm^{-3} because the critical densities of these lines are about 10^6 cm^{-3}. Metallicities in excess of 10^{-2} of solar further raise the CO emissivities, even though the higher abundances of C, O, Si and Fe also enhance the cooling of the gas (Santoro & Shull 2006). The CO emissivities below 10^{-3} solar are negligible.

One finds from Figure 2 that, at a metallicity $> 10^{-2}$ solar, rest frame CO line intensities reach $\sim 10^{-3}$ erg cm^{-2} s^{-1} sr^{-1}, which yields a flux density of $\sim 1.4/(1+z)^3$ Jy for a $0.2''$ source size, or 850 pc at $z = 10$, and a fiducial galaxy center velocity dispersion of 20 km/s. For the rest frame peak in the CO line spectral energy distribution (SED) at 3000 GHz (see Figure 2), 10 km/s velocity resolution and for $z = 10$, ALMA detects such a source at 5σ in 8 hours of integration (50 antennas, beam size = source size). Spectrally resolved detection is possible. ALMA covers 0.3 to 3.0 mm, fortuitously matching most of the X-ray driven CO line SED for $z = 5 - 20$.

4. Discussion

Figure 2 shows how the rest frame spectral line distribution of CO, pure rotational H_2 and H_3^+ evolves with irradiation and metallicity for an ALMA beam that is filled with 1 pc clouds at $\sim 10^5$ cm^{-3}. These clouds are in Keplerian orbit around the central black hole and are randomly distributed over a spherical region with a linear size of 1 kpc in such a way that there is about one cloud along each line of sight. This central region is slowly enriched in metals as indicated. The total column density is on average $\sim 10^{23.5}$ cm^{-2} along each line of sight. The total intensity is then found by a ray-trace on the level populations of the individual clouds. More complicated geometries are not an issue as long as the cloud covering factor is of the order of unity and the bulk of the emitted X-rays are absorbed.

Overall, X-ray fluxes of > 1 erg s^{-1} cm^{-2}, corresponding to black hole masses of $> 10^5$ $M_\odot$ and a region with a size of > 600 pc yield detectable lines, provided the black hole is radiating at its Eddington luminosity. This mass value is comparable to that of black holes present in in cosmological simulations of $10^8 - 10^9 M_\odot$ halos collapsing at $10 < z < 20$

(Peluppessy et al. 2007). Black holes that are emitting below the Eddington luminosity by a factor of x are detectable with ALMA only if their masses exceed $10^5 x\ M_\odot$. Also, the Eddington time of $\sim 10^8$ yr is 25% of the Hubble time at $z = 10$, yielding a fair probability for detection of these systems in the ALMA frequency window. Finding sources is best done in the continuum (e.g. the James Webb Space Telescope), with ALMA follow-up. Since the molecular lines are optically thin, they trace the kinematics of all irradiated gas. Multiple CO and H_2 lines further allow one to determine the ambient density, temperature and X-ray flux.

[OI] 63 μm and [CII] 158 μm fine-structure lines can be important coolants of X-ray irradiated gas as well. At a metallicity of $\sim 10^{-2}$, fine-structure line cooling contributes about half of the total cooling. These lines could also be observed with ALMA, but FUV or cosmic ray irradiation boosts them as well (Meijerink et al. 2007), diminishing their diagnostic value for tracing black hole accretion. In addition, the 149 μm ($J = 1 - 0$, $v = 0$) rotational line of HeH^+ is shown in Figure 2, because it was suggested by Maloney et al. (1996) as a useful XDR tracer. It is found that this line is typically much weaker than the H_2 and CO lines, and HeH^+ abundances do not exceed 10^{-9}.

Fast ($\sim$ 50 km/s) shocks can lead to similar CO and H_2 emissivities, albeit over much smaller regions so that beam dilution would be an issue. Also, shocks should produce CO line profiles with strong non-Gaussian wings. At redshifts of a few, CO emission with upper levels $J = 2 - 10$ from massive tori in active galaxies is also accessible to ALMA. This has been studied by Kawakatu et al. (2007) for the case where FUV photons drive the chemistry. Narayanan et al. (2008a) look at simulations of $z \sim 6$ quasars in $10^{12} - 10^{13}\ M_\odot$ halos and find that the CO is highly excited by starbursts, peaking at $J = 5 - 8$. Narayanan et al. (2008b) further find that AGN-driven winds may leave signatures in the CO line emission profile in the form of high velocity peaks at a few times the circular velocity. Also, Lintott & Viti (2006) and Meijerink et al. (2007) find an increase in HCN emission with X-ray flux, but this effect is suppressed at low metallicity and for densities $\geq 10^5$ cm^{-3}. The X-ray driven lines presented here complement these efforts. Finally, Figure 3 shows a CO comparison between an AGN (XDR) and a starburst (PDR = photon dominated region) model, for the same impinging flux by energy of 100 erg s^{-1} cm^{-2}, typical of a 10^{44} erg s^{-1} Seyfert nucleus or 10^6 B0 stars within a 200 pc region. Solar metallicity is assumed, merely because it favors the PDR. It is obvious that star formation can never compete with an XDR, for the same illuminating flux by energy, in terms of the very high J CO line intensities that are produced.

The authors are grateful to Paul van der Werf for his comments on H_3^+ destruction, to Joe Silk for discussions on CO emission and to the anonymous referee for his/her very helpful comments.

REFERENCES

Abel, T., Bryan, G.L., & Norman, M.L., 2000, ApJ, 540, 39

Bromm, V. & Loeb, A., 2003, ApJ, 596, 34

Bromm, V., Coppi, P.S., & Larson, R.B., 1999, ApJ, 527, L5

Cazaux, S. & Spaans, M., 2004, ApJ, 611, 40

Daddi, E., Dickinson, M., Morrison, G., Chary, R., et al., 2007a, ApJ, 670, 156

Daddi, E., Alexander, D.M., Dickinson, M., Gilli, R., et al., 2007b, ApJ, 670, 173

Di Matteo, T., Springel, V., & Hernquist, L., 2005, Nature, 433, 604

Faure, A., Wiesenfeld, L., Valiron, P., & Tennyson, J., 2006, Phil. Trans. R. Soc., 364, 3113

Ferrarese, L. & Merritt, D., 2000, ApJ, 539, L9

Haiman, Z., Rees, M.J. & Loeb, A., 1997, ApJ, 476, 458

Häring., N. & Rix, H.-W., 2004, ApJ, 604, L89

Kawakatu., N., Andreani, P., Granata, G.L., & Danese, L., 2007, ApJ, 663, 924

Koushiappas, S.M., Bullock, J., & Dekel, A., 2004, MNRAS, 354, 292

Lintott, C. & Viti, S., 2006, ApJ, 646, L37

Lodato, G. & Natarajan, P., 2007, MNRAS, 374, 590

Magorrian, J., Tremaine, S., Richstone, D., Bender, et al., 1998, AJ, 115, 2285

Maloney, P.R., Hollenbach, D.J., & Tielens, A.G.G.M., 1996, ApJ, 466, 561

Mathis, J.S., Rumpl, W., & Nordsieck, K.H., 1977, ApJ, 217, 425

Meijerink, R. & Spaans, M., 2005, A&A, 436, 397

Meijerink, R., Spaans, M. & Israel, F.P., 2006, ApJ, 650, L103

Meijerink, R., Spaans, M. & Israel, F.P., 2007, A&A, 461, 793

Mo, H.J., Mao, S. & White, S.D.M., 1998, MNRAS, 295, 319

Narayanan, D., Li, Y., Cox, T.J., Hernquist, L., et al., 2008a, ApJS, 174, 13

Narayanan, D., Cox, T.J., Brandon, K., et al., 2008b, arXiv:0710.0384

Pan, F.-S. & Oka, T., 1986, ApJ, 305, 518

Pelupessy, F.I., Di Matteo, T., & Ciardi, B., 2007, ApJ, 665, 107

Poelman, D.R. & Spaans, M., 2005, A&A, 440, 559

Poelman, D.R. & Spaans, M., 2006, A&A, 453, 615

Portegies Zwart, S.F., Baumgardt, H., Hut, P., Makino, J., & McMillan, S.L.W., 2004, Nature, 428, 724

Santoro, F. & Shull, J.M., 2006, ApJ, 643, 26

Silk, J., 2005, MNRAS, 364, 1337

Silk, J. & Rees, M., 1998, A&A, 334, L1

Spaans, M. & Silk, J., 2006, ApJ, 652, 902

Woodall, J., Agúndez, M., Markwick-Kemper, A.J., & Millar, T.J., 2006, A&A, 466, 1197

Wyithe, J.S.B. & Loeb, A., 2003, ApJ, 595, 614

Yoshida, N., Sokasian, A., Hernquist, L., & Springel, V., 2003, ApJ, 598, 73

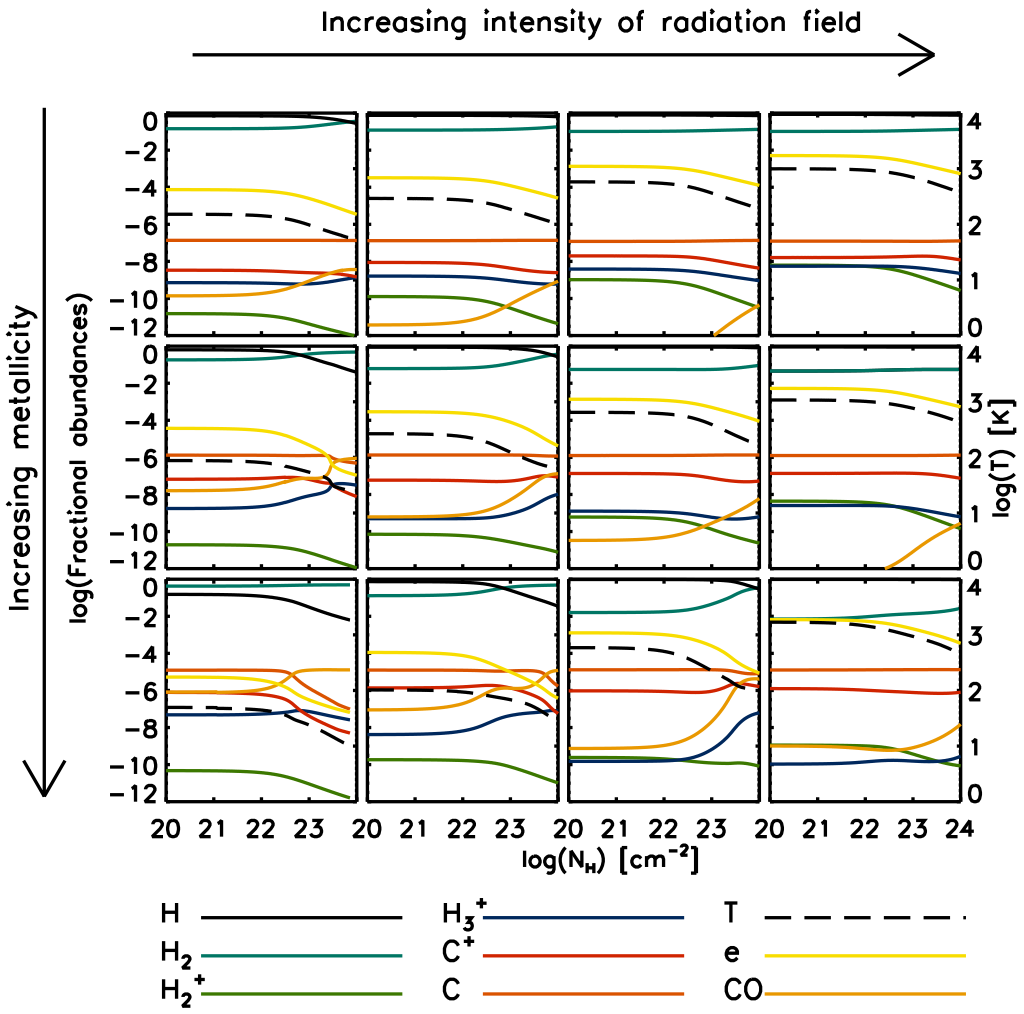

Fig. 1.— Depth dependence of CO, H_2, H_3^+, electron abundance, temperature and other relevant species for various black hole environment models at a density of 10^5 cm^{-3}. The impinging X-ray flux takes on values of 0.1, 1, 10 and 100 erg s^{-1} cm^{-2}; and the metallicity values of 10^{-3}, 10^{-2} and 10^{-1} of solar.

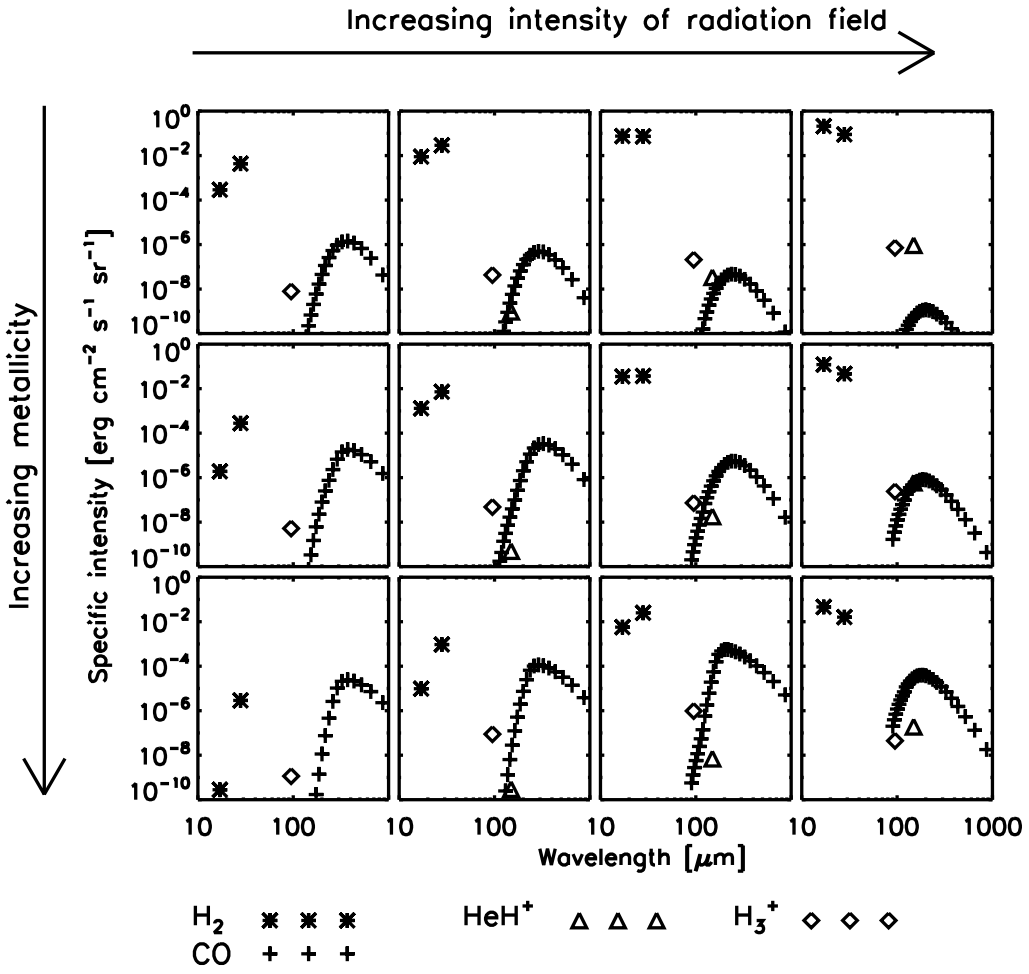

Fig. 2.— Rest frame spectral line distributions of high J CO, H_2 S(0) & S(1), H_3^+ 95 μm and HeH^+ 149 μm are shown as functions of metallicity and X-ray flux for a density of 10^5 cm^{-3}. The impinging X-ray flux takes on values of 0.1, 1, 10 and 100 erg s^{-1} cm^{-2}; and the metallicity values of 10^{-3}, 10^{-2} and 10^{-1} of solar.

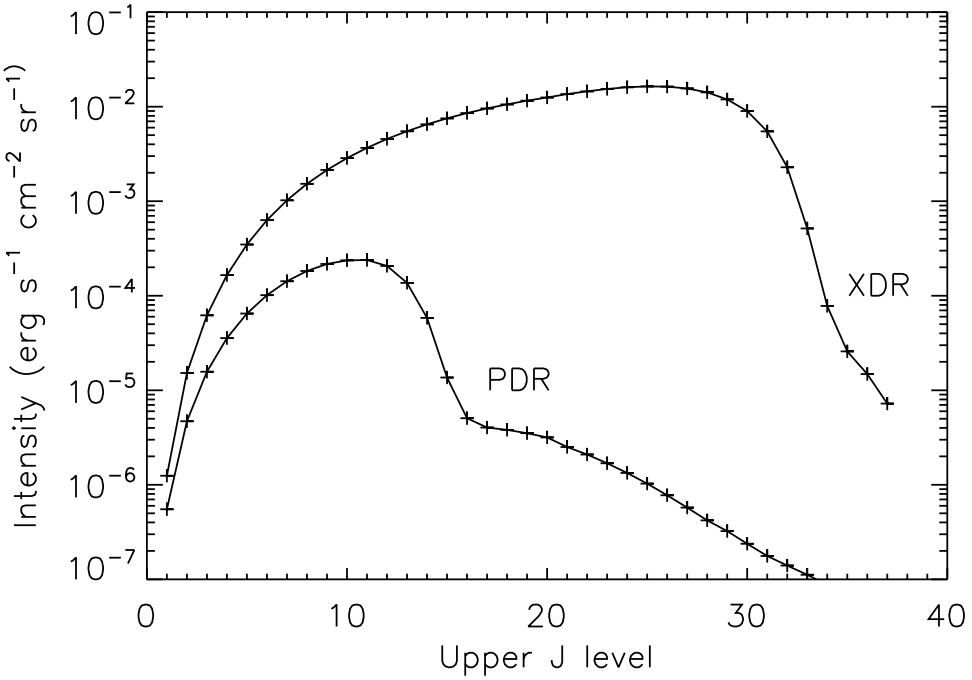

Fig. 3.— Comparison between an AGN and starburst model, for the same impinging flux by energy of 100 erg s^{-1} cm^{-2}, a density of 10^5 cm^{-3} and solar metallicity. The stellar spectrum corresponds to a 30,000 K black body.